INT. J. REMOTE SENSING, 1998, VOL. 19, NO. 8, 1501–1518

Principal component analysis of stacked multi-temporal images for the monitoring of rapid urban expansion in the Pearl River Delta

X. LI†

Centre of Remote Sensing and GIS, Guangzhou Institute of Geography, Guangzhou 510070, P.R. China

A. G. O. YEH

Centre of Urban Planning and Environmental Management, University of Hong Kong, Pokfulam Road, Hong Kong

(*Received 27 February 1997; in final form 5 January 1998*)

Abstract. The Pearl River Delta is experiencing very fast urban growth in recent years which has caused rapid loss of the valuable agricultural land in this fertile region. There is a great need to monitor the rapid urban expansion using remote sensing for urban planning and management purposes. However, it has been well recognized that there is significant over-estimation of land use change in using multi-temporal images for change detection because of inadequate creation of classification signatures. This paper presents a principal component analysis of stacked multi-temporal images method to reduce such errors. The study demonstrates that this method can reduce errors in change detection using multi-temporal images and provide a very useful way in monitoring rapid land use changes and urban expansion in the Pearl River Delta and other parts of the world.

1. Introduction

The launching of Landsat in 1972 began an era of major advancement in the inventory of resources and the monitoring of the environment from space. Since then, techniques have been developed in using satellite images to detect land use change to find out the type, amount, and location of land use change that has taken place. Many applications of using remote sensing data have been documented in the monitoring of land use change in the 80s and 90s (Howarth 1986, Martin 1986, Fung and LeDrew 1987, Eastman and Fulk 1993, Adams *et al.* 1995, Jensen *et al.* 1993, 1995).

A common method for the detection of land use change is to compare two or more dates of images covering the same study area. The detection frequently employs two basic methods—pixel-to-pixel comparison and post-classification comparison (Martin 1989). The first method is a pixel-to-pixel combination of multi-date images without classifying the data. This pixel-to-pixel method has two major types of variations—image differencing (Toll *et al.* 1980) and image ratioing (Nelson 1983). Prior classification is not necessary for the comparisons and errors from classification can therefore be avoided. Unfortunately, the results of these methods could not show the land use conversion matrix. Although they are sensitive in detecting a pixel that

† The author is a post-doctoral fellow of the Centre of Urban Planning and Environmental Management, University of Hong Kong, from January 1997 to December 1998.

has changed, the conversion matrix of land use change cannot be generated from the results. The second method compares two or more separately classified images of different dates. Prior classification is carried out before making the comparison. The advantage of this technique is that the land use types for each pixel of both dates are identified. This post-classification comparison can be used to identify not only the amount and location of change but also the nature of change (Howarth and Wickware 1981). Fung and Zhang (1989) indicate that the comparison is still subject to the error originated from the mis-classification of the two or more independent classified images. Although the use of unsupervised classification for each data set is an ideal independent analysis, this technique cannot produce the highest classification accuracy and lead to the most detailed classification (Johnson and Howarth 1989).

Another method is mask detection which is the combination of pixel-pixel comparison and post-classification comparison (Pilon *et al.* 1988). It attempts to minimize the classification error as much as possible. It is found that change detected by the comparison of classification is easily overestimated and unsatisfactory. The analysis is easily affected by mis-classification and mis-registration errors that may be presented in each classification. Therefore, Pilon *et al.* (1988) propose a masking detection method which excludes unchange pixels from classification in order to reduce classification errors. The first step is to use an overlay enhancement of band-5 images to isolate change pixels. Training areas are created over the areas where the intensity of change is visually determined to be the highest. Classification is produced with a maximum likelihood classifier. Then, a binary change mask is constructed from the classification result. This change mask will later be used to sieve out the change themes from the land use/cover maps produced for each date. In general, the change mask technique can identify change with a higher accuracy than comparable classification approaches. However, it cannot exclude the mis-classification within the change-detected areas since it still uses conventional classification methods.

Other types of change detection techniques have also been reported (Jensen 1996). One of such techniques include principle component analysis which is used frequently in change detection (Fung and LeDrew 1987, Eastman and Fulk 1993). However, Jensen (1996) indicates that this technique has difficulty in trying to interpret and label each component image and to obtain from-to change class information. Therefore, post-classification detection is still considered as one of the most appropriate and commonly used methods for change detection (Jensen *et al.* 1993, Jensen 1996). This paper attempts to use principal component analysis of stacked multi-temporal images to overcome these problems.

2. Methodology

Poor classification accuracy in change detection leads to inaccurate information on land use change. Over-estimation of land use change has been reported due to poor accuracy of classification (Fung and LeDrew 1987). It may be argued that over-estimation mainly comes from inappropriate creation of signatures in classification. In the detection of land use change from images of two dates, the conventional post-classification comparison technique is to classify these images separately. Since the natural environment may change, this method has problems in creating a comparable classification standard for the same class of land use in these two separate images. For example, if an object remains unchanged from time i to time j, it will be very difficult to devise suitable signatures for this object in obtaining the same classification results from two independent classifications from the two images. The spectral features of this object will likely change from image to image because of the influences of atmospheric radiation and the change of sensor's position and solar evaluation angle. Although the target is the same, the detected results may be different due to classification errors. The standards of these two separate classifications are not concordant and thus lead to over-estimation of land use change. Artificial change classes may also be deduced from the conversion matrix due to classification errors, e.g., the change from built-up areas to cropland. One way to avoid the over-estimation of change and other inadequacies is to put these two images together and create a consistent signature for a change class. The disconcordance can be significantly reduced and the over-estimation of change can be largely minimized if the signature of a class is built simultaneously. Instead of classifying X_i and X_j separately, these images are classified simultaneously in obtaining change classes.

For this purposes, a principal component analysis (PCA) of stacked multi-temporal images method is proposed to overcome the over-estimation of land use change and to improve the accuracy of land use change detection. There are four basic steps in this method (figure 1).

2.1. *Stacking images*

Suppose there are two images dated time i and time j available for the detection of land use change. These two images can be referred as two pixel vectors:

$$X_i = [X_{i1}, X_{i2}, \dots X_{in}] \tag{1}$$

and

$$X_j = [X_{j1}, X_{j2}, \dots X_{jn}] \tag{2}$$

where X_{i1} to X_{in} and X_{j1} to X_{jn} are the brightness of the pixel X in bands 1 to n for time i and time j respectively. The first step of this method is to stack the two vectors into one single vector:

$$X = [X_{i1}, X_{i2}, \dots X_{in}, X_{j1}, X_{ij2}, \dots X_{jn}] \tag{3}$$

2.2. *Compressing the stacked image using principal components analysis (PCA)*

This vector consisting of a total of $2n$ bands is difficult to be handled because the size of the data set is too large. Too many bands involved can make the operation of supervised training difficult since the training usually employs a color composite of three bands. It is also found that multi-spectral remote sensing data exhibit high inter-band correlation (Fung and LeDrew 1987). There is a certain degree of redundancy which will lead to high cost for classification if all the data are used. There is a need to compress the data into fewer dimensions. The most commonly used technique for compressing remote sensing data is principal components analysis. The principal components can be standardized by a correlation matrix instead of a covariance matrix (Singh and Harrison 1985, Fung and LeDrew 1987). Both Fung and LeDrew (1987) and Eastman and Fulk (1993) indicate that standardized PCA has a better alignment along the object of interest and appears to be more effective than unstandardized PCA for change detection.

The first principal component stores the maximum contents of the variance of the original data set. The second principal component describes the largest amount

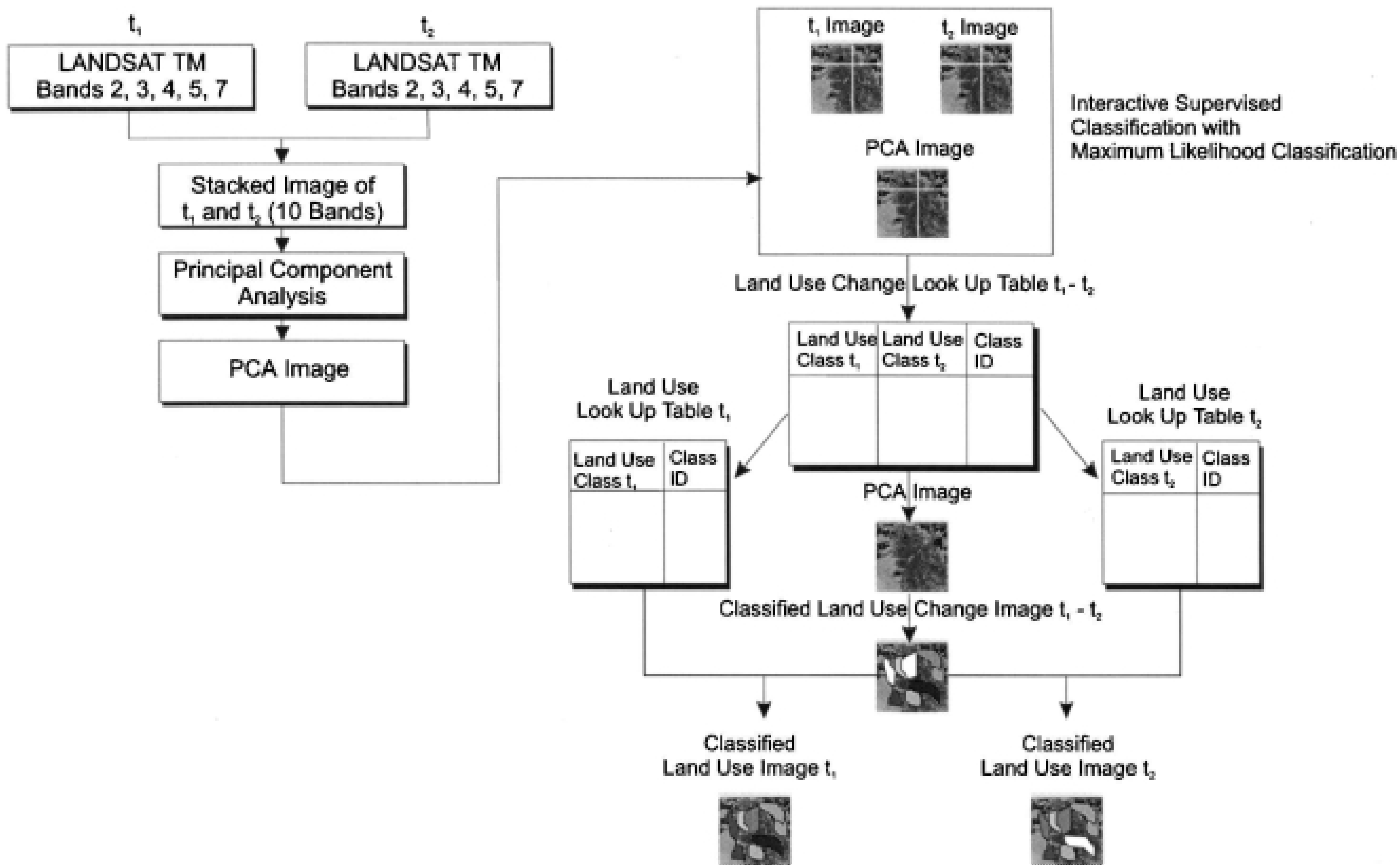

Figure 1 Principal Component Analysis of stacked multi-temporal images with interactive supervised classification in land use change

of the variance in the data that is not already described by the first principal component, and so forth (Taylor 1977). Although n number of principal components may be acquired in the analysis, only the first few principal components account for a high proportion of the variance in the data. In some situations, almost 100 per cent of the variance can be captured by these few components. Fung and LeDrew's study (1987) indicates that the first four components can contain more than 95 per cent of the total variance and the other remaining components have little useful information for land use change.

2.3. *Interactive supervised training on linked images*

Interactive supervised classification of land use change will be carried out on the compressed image created by principal components analysis. As the compressed PCA image contains most of the information of the original images, it should be possible to use the image for the classification of land use change. The signature of each class can be created by interactive supervised training. In the classification, it is important that training samples should be as representative as possible for each class. The samples for supervised classification are selected on the compressed PCA image by displaying the two original images and the compressed PCA image on the screen while using a cursor to pick up training sites. The two original images which are live linked to the PCA image are just used to assist the identification of training samples for land use change class in the PCA image. Actually, the training only needs to pick up 'from–to' change classes which is present in the PCA image by comparing these three linked images. Decomposing can be later carried out to obtain land use classes of the two original images.

Change classes have to be discernable in the PCA image for the training. The original images need to be shown for providing useful information in identifying change classes. Fortunately, all the change classes of the study area can be identified in the PCA image (see figure 4). The next step is to perform a maximum likelihood classification on this compressed components image based on the supervised training. A thematic image containing the information of land use and land use change is produced from the classification.

2.4. *Decomposing the classification result*

The classified image is related to a look-up table recording the information of each class of land use change. The look-up table can be used to construct the land use conversion matrix. Individual pixels can be coded in a change map to identify very specific 'from–to' changes according to the conversion matrix (Jensen *et al.* 1993). In addition, this look-up table can also be decomposed into two separate thematic images which contain the land use class of time i and j. This procedure is opposite to the post-classification comparison method which carries out land use classification for each image before change detection.

Finally, accuracy assessment is needed to test the accuracy of change detection from the classification of satellite images. Many studies have focused on the proper sampling scheme and standard techniques for the assessment (Hord and Brooner 1976, Congalton 1991). The most common way to represent the accuracy is in the form of an error matrix which can be used as a starting point for a series of descriptive and analytical statistical analysis. Sampling needs to be carried out to obtain the error matrix. Random sampling for accuracy assessment can be used to compare the results of change detection and the ground truth which can be obtained from aerial photographs and field checking. Stratified random sampling is usually recommended so that the sampling points are fairly spread in each land use change category (Congalton 1991). This is better than a purely random sampling which may ignore many smaller categories. An error matrix that indicates the concordance of the results of change detection and the ground truth can be constructed from the comparison. Many measurements have been proposed to improve the interpretation of the meaning of the error matrix. Among these methods, the Kappa coefficient is one of the most popular measures in addressing the difference between the actual agreement and chance agreement (Cohen 1960, Campbell 1987, Fung and LeDrew 1988, Congalton 1991).

The Kappa coefficient of agreement is defined as follows:

$$K = \frac{M \sum_{i=1}^{r} X_{ii} - \sum_{i=1}^{r} X_{i+} X_{+i}}{M^2 - \sum_{i=1}^{r} X_{i+} X_{+i}} \tag{4}$$

where r is the number of rows in the error matrix, X_{ii} is the number of observations in row i and column i (the diagonal elements), X_{i+} and X_{+i} are the margin totals of row i and column i respectively, and M is the total number of observations.

3. The detection of land use change in Dongguan in 1988–93

Dongguan is located north of Hong Kong and Shenzhen and south of Guangzhou at the eastern side of the Pearl River Delta (figure 2). The city has a total area of 2465 km^2 consisting of a city proper and 29 towns (figure 3). Like many new cities in the Delta, Dongguan is a fast growing city which was just upgraded to a city from an agricultural county in 1985. The average industrial growth rate was 37 per

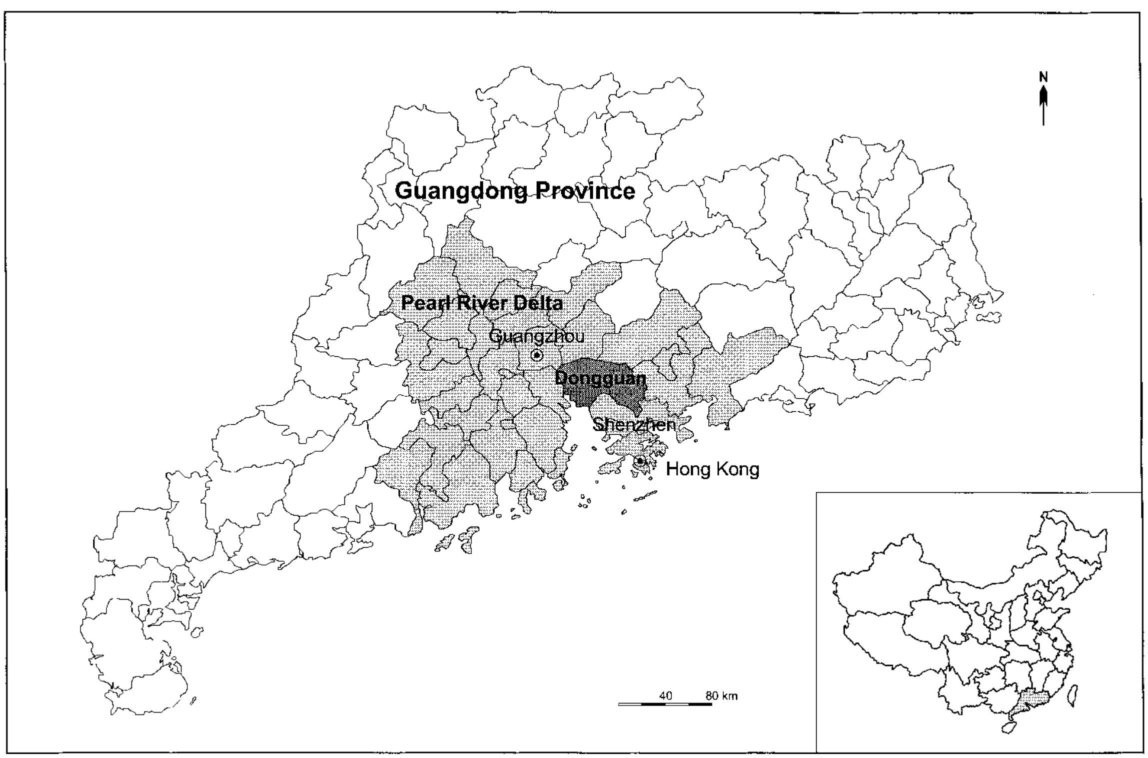

Figure 2. Location of Dongguan in the Pearl River Delta.

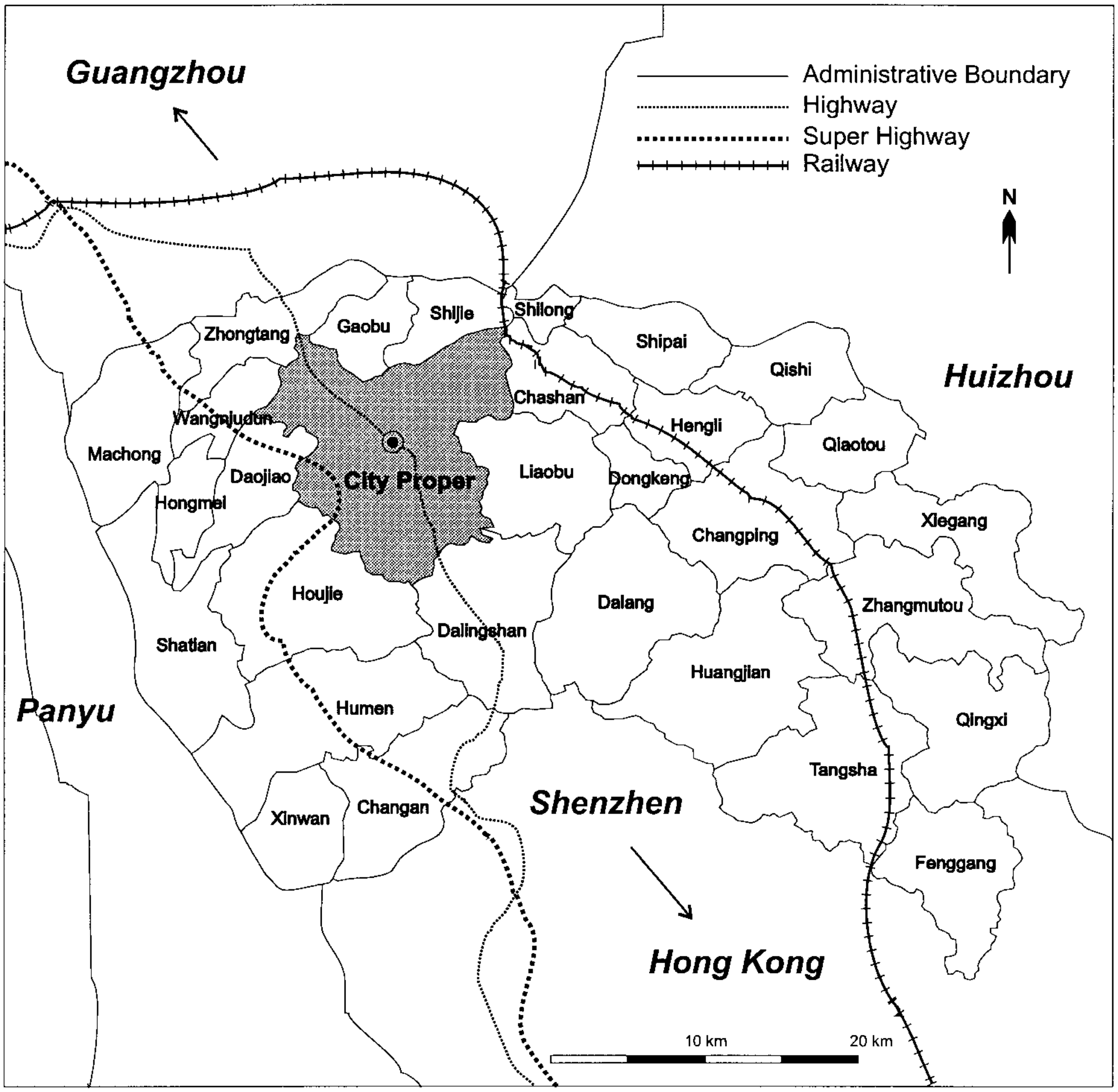

Figure 3. Towns of Dongguan.

cent per annum in 1985–92, with some years as high as over 45 per cent. Concomitant to economic development is rapid urban growth which has caused the encroachment of urban development on the valuable agricultural land. Land development has especially been rapid after 1990 because of the sudden property boom and land speculation in the Pearl River Delta that was fueled by the property boom in Hong Kong.

There are concerns on whether the rapid economic growth in the Pearl River Delta will cause excessive conversion of valuable agricultural land into non-agricultural use. Although it is easy to perceive that there is rapid land use change, detailed and up-to-date land use information is not available. The application of remote sensing can provide a fast and efficient method to inventory land resources and evaluate the environmental impacts of urban development (Yeh and Li 1997). This method is very useful for planners and government officials who would like to monitor and control such rampant development but lack information on the fast growth pattern.

The whole Dongguan administrative area fits into a single Guangzhou Landsat

TM scene (No. 122-44 in China Remote Sensing Ground Station reference system) which has a ground area of 180 km by 180 km. The multi-date images dated 10 December 1988 and 22 November 1993 were obtained for the monitoring of land use change in Dongguan. Sub-scenes covering the whole Dongguan were extracted from these images. Five bands were selected in these images, including band-2, band-3, band-4, band-5 and band-7. Band-1 on the either dates is unavailable due to severe atmospheric attenuation. The natural changes between the two images are minor because the seasons in taking these two images are the same.

The sensor platform, atmosphere, the curvature and rotation of the Earth, and the solar evaluation angle can produce distortions in these remote sensing data. Before using these images in the analysis, such distortions need to be eliminated through image processing. Atmospheric correction and geometric correction are the two basic types of image processing that are needed to correct the image data before any further detailed analysis is carried out.

First, when time series of data are used, it is necessary to remove atmospheric effects on remote sensing data so that they can be comparable. Since atmospheric calibration data were not available for the TM images of the study area, training areas known to be temporary invariant were used for the radiometric rectification (Adams *et al.* 1995). All the data were converted to reflectance values so that the variation in gain and offset between sensors and dates can be removed. The gain and offset was applied to each band of the images to convert digital numbers (DN) to reflectance values. The following formula was used for the conversion (Adams *et al.* 1995).

$$Reflectance = (DN - offset)/gain \tag{5}$$

Second, the registration of the images and maps was performed so that the related images and maps can be overlaid exactly on each other. The procedure of image-to-map registration was to rectify different sources of 'slave' images to a 'master' map using 'ground control points' (GCPs). The conformation is prerequisite to the comparison between separate images, and between images and maps using the same map coordinate system.

In this study, digital relief maps of 1 : 50 000 map scale covering the study area were used as the reference for the registration. The images were rectified to the relief maps using 'ground control points' (GCPs). 25 GCPs were interactively selected across the whole area on each image. Most of the selected GCPs were evenly located at the intersection of roads and rivers. The selection based on the 'well-defined' and 'easily-recognized' points can guarantee the precision of transformation. A second order polynomial transformation equation was established for the rectification based on these control points. The model is:

$$\mathrm{X} = a_0 + a_1 X_0 + a_2 Y_0 + a_3 Y_0 + a_4 X_0 Y_0^2 + a_5 Y_0^2 \tag{6}$$

$$\mathrm{Y} = b_0 + b_1 X_0 + b_2 Y_0 + b_3 X_0 Y_0 + b_4 X_0^2 + b_5 Y_0^2 \tag{7}$$

where X and Y are output map coordinates, X_0 and Y_0 are input image coordinates, and a_i and b_i are the transformation coefficients. The values of the coefficients are listed in table 1. Normally, an acceptable total RMS error is less than 0·5 pixels, or about 15 m on ground (Jensen 1986). The RMS errors of the image-map transformation are listed in table.

The registered 1988 and 1993 images were stacked into one single vector in

Table 1. Coefficients of image-map transformation for the 1988 and 1993 images.

	X	Y
1988		
Constant	2 885·638 255	23 525·651 380
X_0	10·822 945	1·702 790
Y_0	4·926 804	– 10·661 366
X_0^2	0·000 048	– 0·000 047
X_0Y_0	0·000 271	0·000 107
Y_0^2	0·000 117	– 0·000 042
1993		
Constant	1 153·476 819	23 993·759 079
Y_0	11·372 928	– 1·815 958
X_0^2	– 2·342 334	– 11·692 473
X_0Y_0	0·000 051	– 0·000 043
Y_0^2	0·000 183	– 0·000 024

Table 2. RMS errors of image-map transformation for the 1988 and 1993 images (in metres).

	1988	1993
X RMS error	12·2	9·9
Y RMS error	9·2	7·5
Total RMS error	15·3	12·4

ERDAS IMAGINE using the Layer Stack Function. A standardized PCA based on analysis of the correlation matrix was further carried out on the 10-dimensions image (Fung and LeDrew 1987, Eastman and Fulk 1993). The principal components were standardized to zero value mean and unit variance to realize a more effective change detection. The first four components were used in the subsequent analysis since almost all information (97 per cent of the total variance) of the original data had been compacted into these compressed components.

The compressed PCA, 1988 and 1993 images were all displayed on the screen of a Sun workstation. The first three components of the PCA image were displayed as a colour composite on which training samples would be defined. The 1988 and 1993 images were also displayed to assist in identifying the class of each sample. The three images were live linked so that any inquiring cursor at a location on one image would appear at the same location on the other two images (figure 4). This can help a user to interactively define a sample of land use change class on the PCA image by visually comparing these three images with the live link option. For example, in figure 4, the meaning of red tone in the PCA image can be obtained with the interactive supervised training. Sample *A* which is in red in the PCA image can be linked to the same locations in the 1988 and 1993 images. It is easy to identify that the land use of sample *A* in the 1988 image was paddy field while it became construction sites in the 1993 image based on image interpretation. The change class of sample *A* is therefore from paddy to construction sites.

Maximum likelihood classification was performed for the PCA image, producing a thematic image containing the information of land use change. The thematic image was further decomposed into two independent land use images of 1988 and 1993. A

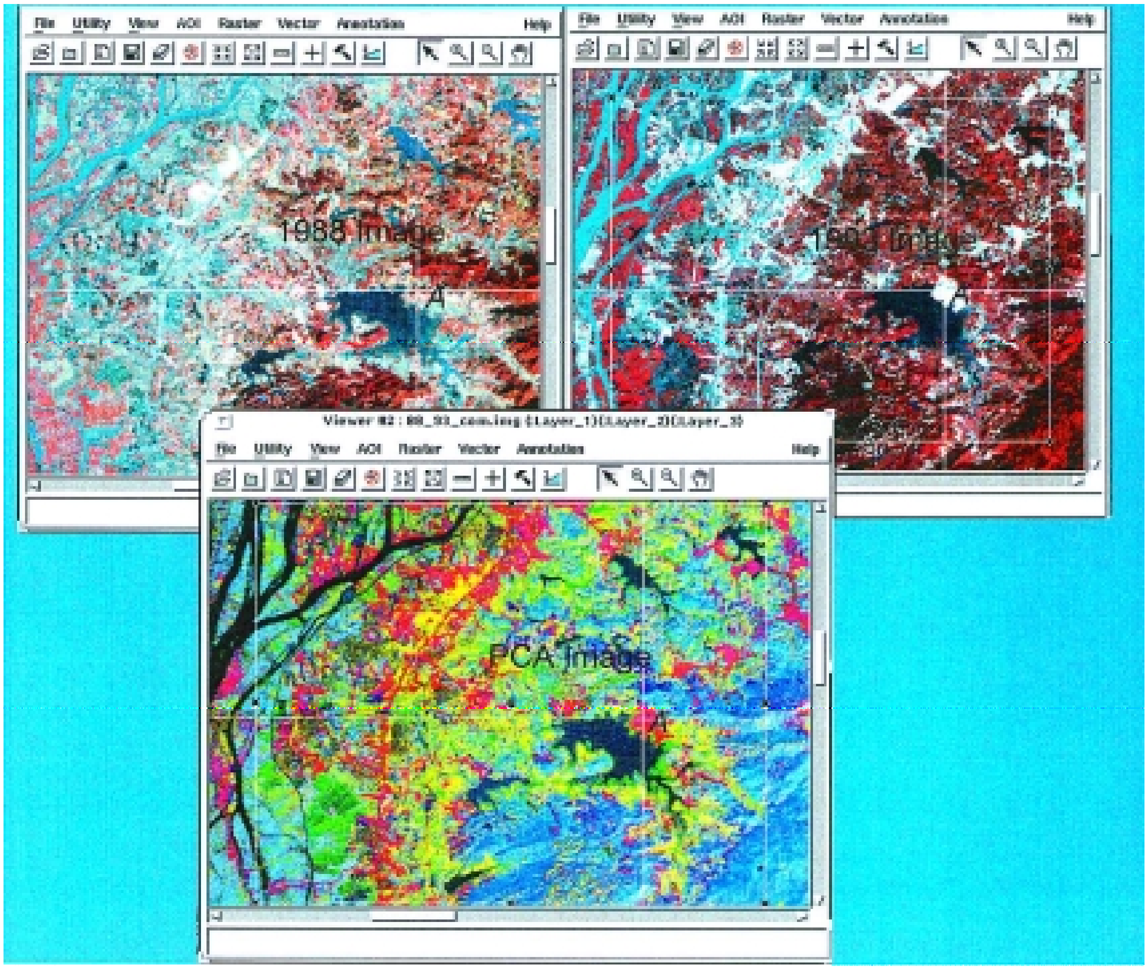

Figure 4. Interactive supervised classification of PCA image for land use change detection.

town mask image prepared from GIS was used to tally the amount of land use change by towns.

Stratified random sampling for accuracy assessment was carried out on the results of the above PCA stacked multi-temporal images method. The sampling method assured that sampling effort was distributed in a rational pattern so that a specific number of observations were assigned to each category on the classified image to be evaluated. Aerial photographs in 1988 and 1993 were used to determine the ground information for the accuracy assessment. Field checking was also carried out to assist the assessment when necessary.

4. Results of change detection

Both land use and land use change in Dongguan were detected using the PCA stacked-image method. The following classes of land use and land use change were identified:

- Cropland
- From barren soil to construction sites
- From water to construction sites
- From cropland to orchard
- From cropland to construction sites
- From construction sites to built-up areas

— Construction sites
— Orchard
— From orchard to construction sites
— From forest to barren soil
— Forest
— Built-up areas
— Water
— From orchard to built-up areas
— From cropland to built-up areas
— From water to built-up areas

Figures 5 and 6 produced by the PCA stacked-image method clearly show the fast urban growth of Dongguan in 1988–93. It can be seen that a significant amount of agricultural land has been encroached by urban expansion. Table 3 is the conversion matrix that shows the land use changes in Dongguan in 1988–93. There are two broad types of land use conversion—the conversion from agricultural land (cropland and orchard) into urban land use (construction sites and built-up areas) and the conversion from cropland into orchard.

There is a significant loss of agricultural land because much of the land has been converted into construction sites. The diminishing rate of agricultural land are surprisingly high when compared with those of other regions in China. Table 4 shows

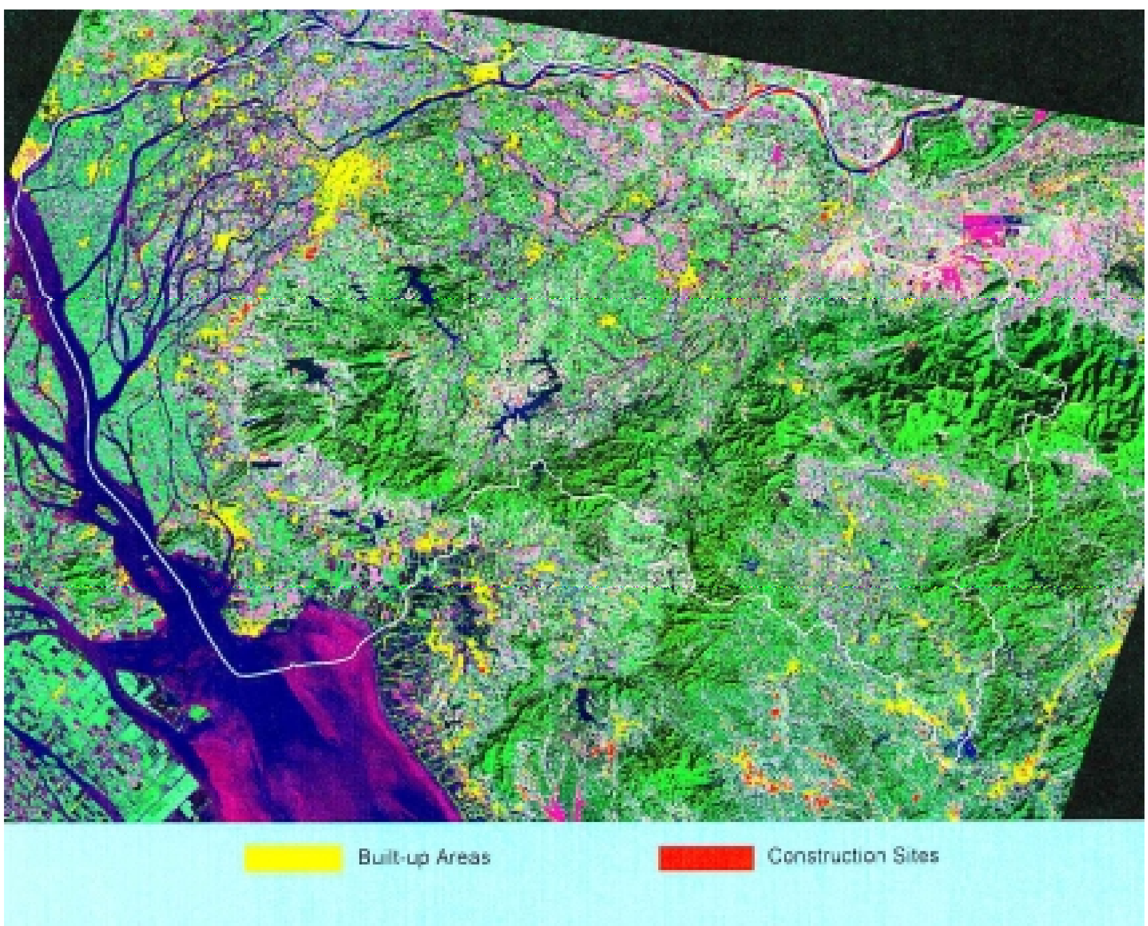

Figure 5. Urban areas (built-up areas and construction sites) of Dongguan in 1988 from the PCA stacked-images method.

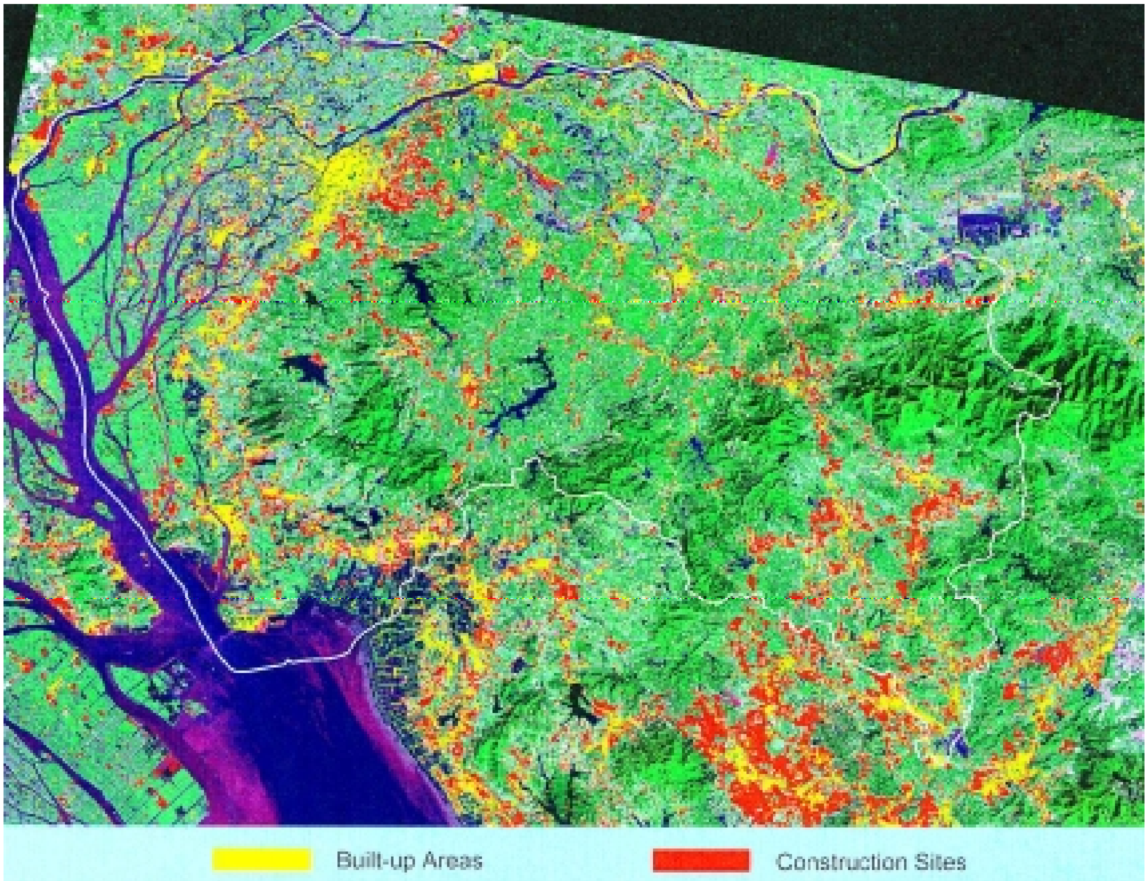

Figure 6. Urban areas (built-up areas and construction sites) of Dongguan in 1993 from the PCA stacked-images method.

Table 3. Land use conversion matrix in Dongguan in 1988–93 (in hectares).

	1993							1988
1988	Cr	Ba	Co	Or	Bu	Fo	Wa	Total
Cr	62 602·4 (64·9%)		1737·8 (1·8%)	31 945·8 (33·1%)	103·2 (0·1%)			96 389·2 (100%)
Ba				0·2 (100%)				0·2 (100%)
Co			0·3 (0·0%)		2115·3 (100%)			2115·6 (100%)
Or			19 432·0 (29·7%)	45 987·9 (70·3%)	9·3 (0·0%)			65 429·2 (100%)
Bu					16 235·8 (100%)			16 235·8 (100%)
Fo		136·7 (0·3%)				41 462·1 (99·7%)		41 598·8 (100%)
Wa			1442·9 (8·0%)		3·4 (0·0%)		16 590·4 (92·0%)	18 036·7 (100%)
1993 Total	62 602·4	136·7	22 613·0	77 933·9	18 467·0	41 462·1	16 590·4	239 805·5

Cr—Cropland, Ba—Barren soil, Co—Construction sites, Or—Orchard, Bu—Built-up areas, Fo—Forest, Wa—Water.

the amount of agricultural land loss in the towns of Dongguan in 1988–1993. It is found that 15·1 per cent of total agricultural land was lost due to rapid urban development in this period of time. The table indicates that 8·9 per cent of the total land area of the city was converted into construction sites and built-up areas. In this table, the values above and below one standard deviation from mean are highlighted to facilitate easy identification of towns with 'abnormal' change. It is found that there is obvious spatial variation in the pattern of agricultural land loss as some towns have suffered large percentages of land loss. The percentages were surprisingly high in some towns where more than 20 per cent of agricultural land was lost just within the five years. These towns, such as Qingxi, Tangsha, Fenggang and

Table 4. Agricultural land loss in the towns of Dongguan in 1988–1993 (in hectares).

Town name	Agricultural land loss	Total agricultural land	Total land	Loss (%) in agricultural land	Loss (%) in total land
City proper	**2 941·9**	**12 239·1**	**21 293·1**	**24·0**	**13·8**
Zhongtang	398·5	3 407·0	5 739·4	11·7	6·9
Wangniudun	192·8	*1 970·9*	*3 060·5*	9·8	6·3
Daojiao	421·5	3 285·0	5 245·9	12·8	8·0
Hongmei	159·8	*2 067·4*	*3 191·3*	7·7	5·0
Machong	410·5	4 885·5	8 683·3	8·4	*4·7*
Humen	1 149·5	6 334·8	**12 923·6**	18·1	8·9
Changan	1 018·3	4 799·4	9 548·1	21·2	10·7
Houjie	975·2	**7 258·5**	12 160·6	13·4	8·0
Shatian	709·6	5 408·0	10 442·6	13·1	6·8
Liaobu	774·8	6 341·8	8 362·5	12·2	9·3
Dalingshan	1 060·3	**7 211·9**	10 561·0	14·7	10·0
Dalang	603·1	**9 202·8**	**12 293·8**	*6·6*	4·9
Huangjian	449·6	5 700·2	**13 241·2**	7·9	*3·4*
Zhangmutou	787·8	2 864·2	11 267·0	**27·5**	7·0
Qingxi	**1 553·7**	5 378·0	10 369·3	**28·9**	**15·0**
Tangsha	**2 004·1**	6 886·4	**12 427·7**	**29·1**	**16·1**
Fenggang	1 307·0	4 312·4	7 933·1	**30·3**	**16·5**
Xiegang	428·9	4 503·5	8 746·8	9·5	4·9
Changping	795·7	**7 427·6**	9 975·6	10·7	8·0
Qiaotou	403·2	4 107·0	5 364·1	9·8	7·5
Hengli	294·2	3 771·1	4 785·5	7·8	6·1
Dongkeng	189·5	*1 830·6*	*2 558·2*	10·4	7·4
Qishi	500·5	4 147·4	5 605·0	12·1	8·9
Shipai	307·2	3 901·0	5 291·3	7·9	5·8
Chashan	511·6	3 841·1	5 439·1	13·3	9·4
Shijie	268·4	2 418·1	*3 535·2*	11·1	7·6
Gaobu	144·5	2 609·6	*3 367·5*	*5·5*	*4·3*
Shilong	212·4	*558·2*	*1 262·7*	**38·1**	**16·8**
Xinwan	311·9	*1 855·7*	5 130·3	16·8	6·1
Total	21 285·7	140 524·8	239 805·4	15·1	8·9
Mean	709·5	4 684·2	7 993·5	15·0	8·5
Standard deviation	603·5	2 429·8	4 249·7	8·2	3·7
Coefficient of variation	85·1	51·9	53·2	54·9	43·1

Values in bold are above one standard deviation from mean.
Values in italic are below one standard deviation from mean.

Zhangmutou, are close to Hong Kong and were deeply involved in the rapid development of property market in the early 1990s.

A special phenomenon can be found in Dongguan. Agricultural land in Dongguan is no longer just used to grow grain as more than half of the land has been converted to the growing of fruit trees. In 1993, the average proportion of land used to grow fruit trees amounted to 55 per cent of the total agricultural land. It is found that the proportion for growing fruit trees is extraordinarily high in some towns (table 5). The four towns with the proportion higher than 70 per cent were Machong, Shatian, Huangjian and Zhangmutou.

The change from cropland to orchard is the result of agricultural restructuring. Dongguan used to be an agricultural county before 1985 and growing grain was a dominant type of agricultural land use. Agricultural land was usually allowed to grow grain while other types of agricultural land use were strictly under control. This simple agricultural land use pattern has been faced with great challenges from the market force since economic reform in China in 1978. The reform has brought

Table 5. Change of proportion of cropland and orchard in the towns of Dongguan in 1988–1993 (in hectares).

	1988		1993	
Town name	Cropland	Orchard	Cropland	Orchard
City proper	8926·2 (59%)	6256·0 (41%)	6336·6 (52%)	5903·7 (48%)
Zhongtang	3163·5 (83%)	642·2 (17%)	2340·0 (69%)	1067·1 (31%)
Wangniudun	1763·8 (82%)	379·9 (18%)	1235·7 (63%)	735·2 (37%)
Daojiao	3059·1 (83%)	647·4 (17%)	2271·9 (69%)	1013·2 (31%)
Hongmei	1745·5 (78%)	481·8 (22%)	1036·6 (50%)	1030·8 (50%)
Machong	3888·5 (73%)	1407·4 (27%)	1368·3 (28%)	3517·2 (72%)
Humen	4336·4 (58%)	3148·6 (42%)	3230·6 (51%)	3105·2 (49%)
Changan	3991·1 (69%)	1827·1 (31%)	3142·8 (65%)	1657·1 (35%)
Houjie	4767·3 (58%)	3468·1 (42%)	3276·3 (45%)	3984·0 (55%)
Shatian	4189·9 (68%)	1927·7 (32%)	1516·7 (28%)	3891·3 (72%)
Liaobu	4351·6 (61%)	2765·0 (39%)	2673·1 (42%)	3668·8 (58%)
Dalingshan	3789·1 (46%)	4483·1 (54%)	2346·9 (33%)	4865·0 (67%)
Dalang	5337·3 (54%)	4468·6 (46%)	3131·6 (34%)	6071·2 (66%)
Huangjian	2882·3 (47%)	3267·4 (65%)	1301·6 (23%)	4398·5 (77%)
Zhangmutou	1271·2 (35%)	2381·0 (65%)	753·8 (26%)	2110·6 (74%)
Qingxi	2890·9 (42%)	4041·2 (58%)	1724·6 (32%)	3653·8 (68%)
Tangsha	4165·3 (47%)	4725·8 (53%)	2726·3 (40%)	4160·7 (60%)
Fenggang	2554·4 (45%)	3065·9 (55%)	1656·7 (38%)	2656·6 (62%)
Xiegang	3108·1 (63%)	1824·4 (37%)	2350·9 (52%)	2152·7 (48%)
Changping	4953·5 (60%)	3270·2 (40%)	2779·9 (37%)	4648·1 (63%)
Qiaotou	2553·4 (57%)	1957·1 (43%)	1868·7 (45%)	2238·6 (55%)
Hengli	2652·4 (65%)	1412·9 (35%)	1873·0 (50%)	1898·1 (50%)
Dongkeng	1282·4 (63%)	737·8 (37%)	848·2 (46%)	982·5 (54%)
Qishi	2444·8 (53%)	2203·5 (47%)	1781·5 (43%)	2367·8 (57%)
Shipai	3047·9 (72%)	1160·4 (28%)	2180·6 (56%)	1722·4 (44%)
Chashan	2943·9 (68%)	1408·8 (32%)	1844·3 (48%)	1996·9 (52%)
Shijie	1934·4 (72%)	752·7 (28%)	1606·0 (66%)	812·7 (34%)
Gaobu	2395·9 (87%)	358·2 (13%)	2037·2 (78%)	572·5 (22%)
Shilong	452·3 (59%)	318·2 (41%)	335·4 (60%)	222·8 (40%)
Xinwan	1526·8 (70%)	640·8 (30%)	1026·7 (55%)	829·0 (45%)
Total	96389·2 (60%)	65429·2 (40%)	62602·4 (45%)	77933·7 (55%)

about two major types of land use change—from growing grain to growing fruit and from agricultural use to urban use.

The significant change of landscape has exerted great influences on the result of the principal components analysis. Generally, it is considered that the first or second component will highlight no-change, whereas the later components highlight change (Fung and LeDrew 1987, Richards 1993). The assumption for the pattern is that area of change occupies only a minor proportion of the entire study area. However, the situation is totally different in the case of Dongguan where land use change dominates the entire scene. As a result, the first principal component does not pick up areas of no-change as in other studies. In contrast, it highlights the change from agricultural land use to construction sites which are prevalent in the whole region. The second component picks up the change from construction sites to built-up areas. It is found that areas of no-change are largely loaded in the third component. The fourth component only picks up some minor changes.

5. Comparison of the accuracy of the PCA stacked-image method with the post-classification comparison method

In order to evaluate the performance of the proposed method as compared with the conventional method, such as post-classification comparison method, change detection using the post-classification comparison was also performed using the 1988 and 1993 images. The classification was based on supervised training using the same bands. Table 6 is the conversion matrix created from this method. This method is problematic because a lot of unlikely conversion and over-estimation of change was obtained. For example, the matrix shows that some construction sites and built-up areas were impossibly converted into agricultural land again due to classification errors. 26 per cent of water became land area and 36 per cent of forest area became other types of land uses. Field investigation indicates that most of these detected changes does not exist. Although a GIS mask could be used to remove some of the classification errors in the post-classification method, this technique was not employed for both methods because we would like to demonstrate that the proposed method can produce better accuracy for change detection under similar conditions.

Table 7 is the error matrix constructed from the sampling data using all categories from the PCA stacked-image method. The kappa coefficient is 0·85 and the overall

Table 6. Land use conversion matrix from the post-classification comparison method (in hectares).

	1993							
1988	Cr	Ba	Co	Or	Bu	Fo	Wa	1988 Total
Cr	29 243·3		7 933·6	26 299·2	14 224·6	2 396·7	1 721·5	81 818·9
Ba								
Co	258·0		328·7	327·1	554·1	16·2	115·0	1 599·1
Or	9 653·3		2 890·4	22 012·5	4 081·8	6 164·9	338·2	45 141·0
Bu	11 402·8		1 223·9	3 937·9	10 662·5	769·6	1 397·0	29 394·5
Fo	2 090·2		1 116·7	8 967·0	1 120·1	23 464·7	339·5	37 098·1
Wa	2 913·9		258·3	236·6	1 554·8	520·7	15 067·4	20 551·8
1993 Total	55 561·6		13 751·6	61 780·1	32 197·9	33 332·9	18 979·5	215 603·5

Cr—Cropland, Ba—Barren soil, Co—Construction sites, Or—Orchard, Bu—Built-up areas, Fo—Forest, Wa—Water.

Table 7. Confusion matrix of the PCA stacked-image method.

	Reference data																
Classified data	1.	2.	3.	4.	5.	6.	7.	8.	9.	10.	11.	12.	13.	14.	15.	16.	Total
1. Cr	128			12	4			4				10	6				164
2. Ba to Or		64															64
3. Wa to Co			50		1							2					53
4. Cr to Or	4	4		64				20			2						94
5. Cr to Co			3		90		1			2							96
6. Co to Bu						30									2		32
7. Co					2		36										38
8. Or	10			14	4			76	2		6		2				114
9. Or to Co					10				64								74
10. Fo to Ba										52							52
11. Fo								8			86						94
12. Bu					2							42	4			2	50
13. Wa													56				56
14. Or to Bu														62	4		66
15. Cr to Bu						2								2	54		58
16. Wa to Bu											3					24	27
Total	142	68	53	90	113	32	37	108	66	54	97	54	68	64	60	26	1132

Cr—Cropland, Ba—Barren soil, Co—Construction sites, Or—Orchard, Bu—Built-up areas, Fo—Forest, Wa—Water.

Table 8. Comparison of accuracies between the PCA stacked-image and conventional post-classification comparison methods in the detection of change and no-change.

(*a*) *PCA stacked-images method.*

	Reference data		
Classified data	No-change	Change	Total
No-change	474	42	516
Change	32	584	616
Total	506	626	1132

Kappa coefficient = 0·87.
Overall accuracy = 0·93.

(*b*) *Conventional post-classification comparison method.*

	Reference data		
Classified data	No-change	Change	Total
No-change	360	28	388
Change	134	452	586
Total	494	480	812

Kappa coefficient = 0·66.
Overall accuracy = 0·83.

accuracy is 0·86. Table 8 shows the comparison of accuracy between the proposed method and the conventional post-classification comparison method in the detection of change and no-change. It is shown that quite a large number of unchanged pixels have been classified as changed pixels (134 pixels in the total of 586 pixels) by mistake in the conventional method. This indicates that the proposed PCA stacked-image method is better than the conventional method. The proposed method can significantly minimize over-estimation of land use change. The kappa coefficient is 0·87 for the PCA stacked-image method but is only 0·66 for the conventional method. The PCA stacked-image method can reduce the errors in change detection using multi-temporal images and provide a very useful way in monitoring land use change and urban development.

Acknowledgements

The authors are very grateful for the useful comments received from the anonymous referees for the revision of this paper. This research has been supported by the Hong Kong Research Grants Council.

References

Adams, J. B., Sabol, D. E., Kapos, V., Filho, R. A., Roberts, D. A., Smith, M. O., and Gillespie, A. R., 1995, Classification of multispectral images based on fractions of endmembers: application to land-cover change in the Brazilian Amazon. *Remote Sensing of Environment*, **52,** 137–154.

Campbell, J. B., 1987, *Introduction to Remote Sensing* (New York: The Guilford Press).

Cohen, J., 1960, A coefficient of agreement for nominal scale. *Educational and Psychological Measurement* , **20,** 37–46.

Congalton, R. G., 1991, A review of assessing the accuracy of classification of remotely sensed data. *Remote Sensing of Environment*, **37,** 35–46.

Eastman, J. R., and Fulk, M., 1993, Long sequence time series evaluation using standardized principle components. *Photogrammetric Engineering and Remote Sensing*, **59,** 991–996.

Fung, T., and LeDrew, E., 1987, Application of principal components analysis change detection. *Photogrammetric Engineering and Remote Sensing*, **53,** 1649–1658.

Fung, T., and LeDrew, E., 1988, The determination of optimal threshold levels for change detection using various accuracy indices. *Photogrammetric Engineering and Remote Sensing*, **54,** 1449–1454.

Fung, T., and Zhang, Q., 1989, Land use change detection and identification with Landsat digital data in the Kitchener-Waterloo area. In *Remote Sensing and Methodologies of Land Use Change Analysis* edited by C. R. Bryant, E. F. LeDrew, C. Marois and F. Cavayas (Waterloo: University of Waterloo), pp 135–153.

Hord, R. M., and Brooner, W., 1976, Land use map accuracy criteria. *Photogrammetric Engineering and Remote Sensing*, **42,** 671–677.

Howarth, P. J., 1986, Landsat digital enhancements for change detection in urban environment. *Remote Sensing of Environment*, **13,** 149–160.

Howarth, P. J., and Wickware, G. M., 1981, Procedures for change detection using landsat digital data. *International Journal of Remote Sensing*, **2,** 277–291.

Jensen, J. R., 1986, *Digital Image Processing: a Remote Sensing Perspective* (Englewood Cliffs: Prentice-Hall).

Jensen, J. R., 1996, *Introductory Digital Image Processing: A Remote Sensing Perspective* (Saddle River: Prentice-Hall, Inc.).

Jensen, J. R., Cowen, D. J., Althausen, J. D., Narumalani, S., and Weatherbee, O., 1993, An evaluation of the Coastwatch Change Detection Protocol in South Carolina. *Photogrammetric Engineering and Remote Sensing*, **59,** 1039–1046.

Jensen, J. R., Rutchey, K., Koch, M. S., and Narumalani, S., 1995, Inland wetland change detection in the Everglades Water Conservation Area 2A using a time series of normalized remotely sensed data. *Photogrammetric Engineering and Remote Sensing*, **61,** 199–209.

JOHNSON, D. D., and HOWARTH, P. J., 1989, The effects of spatial resolution on land cover/land use theme extraction from airborne digital data. In *Remote Sensing and Methodologies of Land Use Change Analysis*, edited by C. R. Bryant. E. F. LeDrew, C. Marois and F. Cavayas (Waterloo: University of Waterloo), pp. 117–134.

MARTIN, L. R. G., 1986, Change detection in the urban fringe employing landsat satellite imagery. *Plan Canada*, **26,** 182–190.

MARTIN, L. R. G., 1989, An evaluation of landsat-based change detection methods applied to the rural-urban fringe. In *Remote Sensing and Methodologies of Land Use Change Analysis*, edited by C. R. Bryant, E. F. LeDrew, C. Marois and F. Cavayas (Waterloo: University of Waterloo). pp. 101–116.

NELSON, R. F., 1983, Detecting forest canopy changes due to insect activity using Landsat MSS *Photogrammetric Engineering and Remote Sensing*, **49,** 1303–1314.

PILON, P. G., HOWARTH, P. J., and BULLOCK, R. A., 1988, An enhanced classification approach to change detection in semi-arid environments. *Photogrammetric Engineering and Remote Sensing*, **54,** 1709–1716.

RICHARDS, J. A., 1993, *Remote Sensing Digital Image Analysis: An Introduction* (New York: Springer-Verlag).

SINGH, A., and HARRISON, A., 1985, Standardized principal components. *International Journal of Remote Sensing*, **6,** 883–896.

TAYLOR, P., 1977, *Quantitative Methods in Geography: An Introduction to Spatial Analysis* (Boston, Massachusetts: Houghton Mifflin Company).

TOLL, D. L., ROYAL, J., and DAVIS, J. B., 1980, Urban area update procedures using landsat data *Proceedings of American Society of Photogrammetry*, (Falls Church, VA: American Society of Photogrammetry), pp. RS-1-E-1–RS-1-E-17.

YEH, A. G. O., and LI, X., 1997, An integrated remote sensing and GIS approach in the monitoring and evaluation of rapid urban growth for sustainable development in the Pearl River Delta, China. *International Planning Studies*, **2,** 193–210.